Available online at www.sciencedirect.com
ScienceDirect
ELSEVIER
Catalysis Today 131 (2008) 378–384
CATALYSIS TODAY
www.elsevier.com/locate/cattod

Selective synthesis of *para–para*′-dimethyldiphenylmethane over H-beta zeolite

Dingfeng Jin, Zhaoyin Hou *, Liwei Zhang, Xiaoming Zheng

Institute of Catalysis, Department of Chemistry, Zhejiang University (Xixi Campus), Hangzhou 310028, PR China

---

Abstract

Selective synthesis of *para–para*′-dimethyldiphenylmethane (*para–para*′-DMDPM) from the condensation between toluene and formaldehyde was investigated over H-X, H-Y, H-ZSM-5, H-mordenite and MCM-41. Characterizations (NH_3-TPD-MS and pore structure) disclosed that the catalytic activity of various zeolites depends mainly on its strong acid site and accessibility of the internal pores. H-beta zeolite, with a unique pore sized in 0.66 nm and higher proportion of stronger acid site, exhibited the highest activity and stereo-selectivity (86.5%). Small sized H-beta zeolite was more active due to the enhanced accessibility of its acid site, and this kind of zeolite remained a higher stereo-selectivity (>80%) even at higher temperature, longer reaction time and recycle usage. The best yield of *para–para*′-DMDPM reached 71.1% at 140°C over H-beta zeolite and it could be used in recycle without loss of its structure, activity and stereo-selectivity.

Keywords: H-beta zeolite; Dimethyldiphenylmethane; Toluene and formaldehyde

---

1. Introduction

Dimethyldiphenylmethane ($CH_3PhCH_2PhCH_3$, DMDPMs) is an important chemical and synthetic intermediate in the production of spices, pharmaceutics and dielectric fluid. And diphenylmethane dyes (e.g. auramine) are widely used in wool, paper, leather and silk industries [1]. Conventionally, DMDPMs are synthesized via the condensation between benzyl chloride and *p*-xylene catalyzed by liquid protonic acids (e.g. HCl), which gives large amount of by-products such as polymers of benzyl chloride and several compounds having 3 or more benzene rings (Eq. (1)) [2,3].

$$CH_3C_6H_4CH_3 + C_6H_5CH_2Cl \rightarrow CH_3PhCH_2PhCH_3 + HCl \quad (1)$$

At the same time, the use of homogeneous acid catalysts possesses several problems, such as difficulty in separation and recovery, disposal of spent catalyst, corrosion and high toxicity [4–7]. It is important to develop easily separable and reusable heterogeneous solid acid catalysts having high activity and selectivity for the industrially demanding DMDPMs synthesis process.

Recently, several solid acid catalysts relevant to this kind of condensation reaction have been reported to replace conventional problematic homogeneous catalysts. Those include heteropoly acid [8,9], sulfuric acid functionalized mesoporous MCM silica [10], sulphated zirconia [11,12], zeolite [13] and clays [14]. But these reported heterogeneous catalysts have shown drawbacks such as lower activity or selectivity, formation of higher amount of polyalkylated products and crucial reaction conditions [15,16].

Previous work found that 12-tungstophosphoric acid exhibited high activity for the condensation between benzene and formaldehyde [17,18] and for the condensation of toluene and formaldehyde (Eq. (2)) [19].

$$2C_6H_5CH_3 + HCHO \rightarrow CH_3PhCH_2PhCH_3 + H_2O \quad (2)$$

This process is economical and environmental favorable as the only by-product is water. While the solid state heteropoly acids changed into a slurry state after reaction due to the formation of water, which brought difficulties in the following separation process and the loss of catalyst in the recycle usage [19], and the selectivity of *para–para*′-DMDPM was low [20].

---

* Corresponding author. Tel.: +86 571 88273272; fax: +86 571 88273283.
E-mail address: zyhou@zju.edu.cn (Z. Hou).

0920-5861/$ – see front matter © 2007 Elsevier B.V. All rights reserved.
doi:10.1016/j.cattod.2007.10.049

In this contribution, we want to report the excellent performance of small sized H-beta zeolite at higher toluene/HCHO ratio for the selectively synthesis of *para–para′*-DMDPM. The influences of reaction conditions on the distribution of its isomers over H-beta zeolite and the recycle usage are investigated.

2. Experiment

Three H-beta zeolite with different particle sizes were synthesized following the literature [21], then ion-exchanged (four times) using 0.1 M NH_4Cl (30 ml per 1 g zeolite) at 90 °C to guarantee Na^+ and K^+ complete exchanged by NH_4^+ ions. After washed by distilled water, these samples were dried in air at 100 °C for 24 h, calcined at 550 °C for 3 h and the resulting zeolite were denoted as H-beta-1, H-beta-2 and H-beta-3. Pure-silica MCM-41 was synthesized following a procedure as described in literature [22]. Reference zeolite (H-X, H-Y, H-mordenite, H-ZSM-5) were kindly supplied by Huahua Catalysis Co. (Wenzhou, China) and further calcined at 550 °C for 3 h before catalytic reaction and characterization.

A mixture of toluene (450 mmol), paraformaldehyde (30–90 mmol of HCHO) and nitrobenzene (20 mmol, internal standard) was poured into the catalyst in a custom-designed 150 cm^3 stainless autoclave (Lanzhou, China). And this suspension was vigorously stirred with a magnetic stirrer. After reaction, the reactor was cooled to room temperature; solid catalyst was separated by centrifuging. Organic reactant solution was diluted with ethanol and analyzed using FID gas chromatography spectrometry equipped with a 25 m capillary column of a cross-linked 5% phenylmethylsilicone (HP5988A, USA). All products were confirmed with the standard mass spectrum in database and that of the standard products purchased from TCI (Shanghai Branch, China) in GC–MS (Trace GC 2000/Trace MS with NIST Mass Search V 2.0 database, Finnigan, USA).

The structure of the tested zeolite was carried out at 77.35 K on an Omnisorp Coulter 100CX (USA) analyzer. All samples were degassed at 250 °C for 2 h under high vacuum prior to analysis. BET surface areas were calculated from the linear part of the BET plot. The pore size distributions were calculated using Barret–Joyner–Hallender (BJH) method based on the desorption branch.

X-ray diffraction patterns were obtained with X-ray diffractometer in a D8 ADVANCE (BRUKER, Germany) equipment using nickel-filtered Cu Kα radiation at 40 kV and 40 mA. Diffraction data were recorded using continuous scanning with a rate of 0.01°/s.

Scanning electron microscopy (SEM) images were obtained on the XL-30 (Philips) with an acceleration voltage of 30 kV.

The acidity of the tested zeolite were detected by NH_3 temperature-programmed desorption (NH_3-TPD) in quartz tubular reactor in an auto-catalytic adsorption system (AMI-200, Zeton Altamira, Pittsburgh, USA), using an on-line mass analyzer (OmniStar^{TM}, GSD301, Switzerland). Sample was first pretreated at 500 °C in argon flow for 1 h and then cooled to 50 °C. Ammonia (20% NH_3/Ar) was introduced at a flow rate of 30 ml/min for 0.5 h at 50 °C, then blown by argon; the reactor temperature was programmed to increase at a ramp rate of 10 °C/min, and the amount of ammonia ($m/e = 16$) in effluent was measured and recorded as function of temperature.

3. Results and discussion

3.1. Condensation between toluene and HCHO over various zeolites

Conversion of formaldehyde and selectivity of DMDPMs in the condensation between toluene and formaldehyde over various zeolites are summarized in Table 1. It can be found that no reaction happened on MCM-41. H-X, H-modernite, H-Y and H-ZSM-5 had very low activity and the main products were *ortho–para′*-DMDPM and *para–para′*-DMDPM. H-beta exhibited a higher activity and higher *para–para′*-DMDPM selectivity.

NH_3 temperature-programmed desorption mass spectroscopy (NH_3-TPD-MS) indicated that these catalysts showed a wide range of acid site density and acid strength distributions (Fig. 1). Two NH_3 desorption peaks were detected in the range of 150–400 °C and 400–600 °C, which inferred that two kind of acid sites exist on the surface of these zeolite. According to the published data [23–26], these kinds of adsorbed ammonia species could be assigned to NH_3 weakly adsorbed on the Lewis acid site, NH_4^+ on the Brönsted acid site, and NH_3 strongly adsorbed on and/or interacted with the dislodged Al, respectively. It is interesting to note that the amount of stronger acid site in H-beta is high and the amount of the stronger acid site increases in the order of H-X < H-ZSM-5 < H-modernite < H-Y ≈H-beta, which fits with the order of

Table 1
Conversion and selectivity of DMPMs from toluene and HCHO over various zeolites

Catalysts	Conversion of			Selectivity(on the basis of HCHO) (mol%)[a]		
	HCHO (%)	Toluene (%)	*Ortho–ortho′*	*Ortho–para′*	*Para–para′*	3-Rings
H-X	4.0	0.5	1.0	48.3	50.7	0.0
H-Y	12.4	1.7	2.0	48.6	49.4	0.0
H-beta-1	75.9	10.1	1.1	10.3	86.5	2.0
H-mordenite	4.4	0.6	0.7	54.4	44.9	0.0
H-ZSM-5	13.7	1.8	3.9	52.3	43.8	0.0
MCM-41	0.0	–	–	–	–	–

Reaction conditions: zeolite 2.0 g; toluene 450 mmol; HCHO 30 mmol; reaction time 4 h and 140 °C.

[a] Selectivity of DMDPMs = (mol of DMDPMs)/(total mol of DMDPMs + 2 × mol of 3-rings products) × 100%.

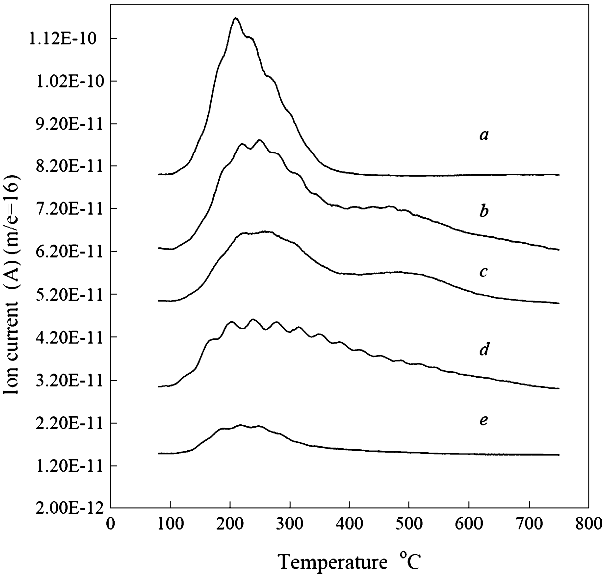

Fig. 1. NH_3-TPD-MS profiles of the different zeolites. (a) H-X (Si/Al = 3), (b) H-Y (Si/Al = 6), (c) H-beta-1 (Si/Al = 10), (d) H-mordenite (Si/Al = 19) and (e) H-ZSM-5 (Si/Al = 25).

their catalytic activity. These results inferred that zeolite with higher proportion of stronger acid sites would be more active for the activation of formaldehyde [19,27].

At the same time, the structure of the these zeolites (Table 2) indicated that H-beta has a unique pore sized in 0.66 nm and a distorted tetrahedral channel structure with three mutually intersecting 12-ring channels in which molecules as large as tetraethyl ammonium cations can enter with ease, which would be fitting better the transition state of the condensation between toluene and formaldehyde. H-ZSM-5 with smaller pore opening (0.56 nm), is poorly active because the diffusion of DMDPM is strongly hindered. For H-mordenite, the presence of one-dimensional channels also causes diffusion problems and therefore, low activity. H-X and H-Y are less active, due to their larger pore spaces is too wide to activate toluene and formaldehyde.

3.2. Influence of the toluene/HCHO ratio and the amount of H-beta

Table 3 shows the conversion of formaldehyde and the products distribution in the condensation between toluene and HCHO at different toluene/HCHO ratio (abbreviated as T/F). It can be found that conversion of formaldehyde increased from 11.3% to 54.3% with the increasing T/F ratio from 5 to 15. And the selectivity of DMDPMs (total of 2-rings products) increased at the same time. Higher T/F ratio is favorable for the selective synthesis of *para–para′*-DMDPM, the formation of 1-ring product fell from 15.0% to 6.8%. Over 2.0 g zeolite, the conversion of HCHO and selectivity of *para–para′*-DMDPM were further increased from 34.1% and 70.6% (at T/F = 5) to 75.9% and 86.5% (at T/F = 15), respectively. Among the 2-rings products, the molar ratio of *ortho–ortho′*, *ortho–para′* and *para–para′* isomers was 1.5/10.3/86.5. This stereo-selectivity is higher than that of previous works [14,19,20,27].

In principle, the micropores of the zeolite could be easily blocked by-products having two and more phenyl rings, which decreased its activity. In order to overcome these problems, high toluene to formaldehyde ratio is more favorable for the reaction and relatively faster diffusion of the products is expected. And also, higher amount of catalyst could also increase the accessibility of acid site and enhance the shape selectivity due to product diffusion.

3.3. Condensation between toluene and formaldehyde over different sized H-beta

Scanning electron micrographs of the as-synthesized H-beta are showed in Fig. 2 and the size distributions are summarized in attached drawings. The detected average particle size of as-synthesized H-beta-1, H-beta-2 and H-beta-3 were 0.3, 0.6 and 1.0 μm. After ion-exchange and calcination (550 °C, 3 h), the detected particle size increased to 0.6, 2.5 and 5.0 μm (Fig. 3). The XRD spectrum of the final H-beta is shown in Fig. 4. Their XRD patterns were qualitatively similar to those reported in the literatures [28,29].

These different sized H-beta zeolites were used in the condensation between toluene with formaldehyde, and their activities are summarized in Table 4. It can be found that small sized H-beta gives higher activity than those in large particle size, which indicates that diffusion has a bigger influence on this reaction even in the large pore of H-beta zeolite [30]. And due to the limitation of diffusion, only a fraction of the acid sites is accessible to the reactants in large sized H-beta, which inferred that their activity would decrease with the increasing particle size.

Table 2
The structure of different zeolites

Zeolites	Code of structure type	Channel system size (nm)[a]	S_{BET} (m^2/g)	Pore diameter		Pore volume (cm^3/g)
				Micropore diameter (nm)	Mesopore diameter (nm)	
H-X	FAU	⟨1 1 1⟩ 12 0.74 × 0.74***	631.9	0.74	–	0.32
H-Y	FAU	⟨1 1 1⟩ 12 0.74 × 0.74***	550.5	0.74	–	0.39
H-beta	BEA	⟨1 0 0⟩ 12 0.66 × 0.67*←→[0 0 1] 12 0.56 × 0.56*	541.1	0.66	–	0.30
H-Mordenite	MOR	[0 0 1] 12 0.65 × 0.70*←→{[0 1 0] 8 0.34 × 0.48 [001] 8 0.26 × 0.57}*	40.4	–	–	0.00
H-ZSM-5	MFI	{[1 0 0] 10 0.51 × 0.55←→[0 1 0] 10 0.53 × 0.56}***	302.6	0.56	–	0.32
MCM-41	–	–	1064.5	–	3.1	0.80

[a] Theoretical data reported [30].

Table 3
Conversion and selectivity of DMPMs at different T/F ratio

Amount of HCHO (mmol)	T/F (M)[a]	Conversion of			Selectivity (on the basis of HCHO) (mol%)[d]			
		HCHO (%)	Toluene (%)	1-Ring	*Ortho–ortho′*	*Ortho–para′*	*Para–para′*	3-Rings
30	15	54.3[b]	6.9	6.8	1.6	15.9	74.1	2.6
60	7.5	27.9[b]	7.1	9.2	3.3	20.3	65.0	2.2
90	5	11.3[b]	4.2	15.0	8.9	33.1	42.0	1.0
30	15	75.9[c]	10.1	0.0	1.1	10.3	86.5	2.1
90	5	34.1[c]	13.2	5.3	1.8	20.5	70.6	1.8

Reaction conditions: catalyst is H-beta-1 zeolite; toluene 450 mmol; reaction time 4 h and 140 °C.

[a] The molar ratio between toluene and formaldehyde.

[b] The amount of H-beta-1 zeolite is 1.0 g.

[c] The amount of H-beta-1 zeolite is 2.0 g.

[d] Selectivity of DMDPMs = (mol of DMDPMs)/(mol of 1-ring products + total mol of DMDPMs +2 × mol of 3-rings products) × 100%.

3.4. Time course of condensation between toluene and HCHO over H-beta

The catalytic performance of H-beta-1 at different reaction time at 140 °C for directly synthesis of DMDPMs via the condensation between toluene and formaldehyde are shown in Fig. 5. It could be found that the conversion of HCHO increased from 52.7% to 82.7% with the increased reaction time from 2 to 6 h. The selectivity of DMDPMs decreased slightly as the amount of consecutive 3-rings products increased with the reaction time, while the selectivity of *para–para′*-DMDPM was above 86.0%.

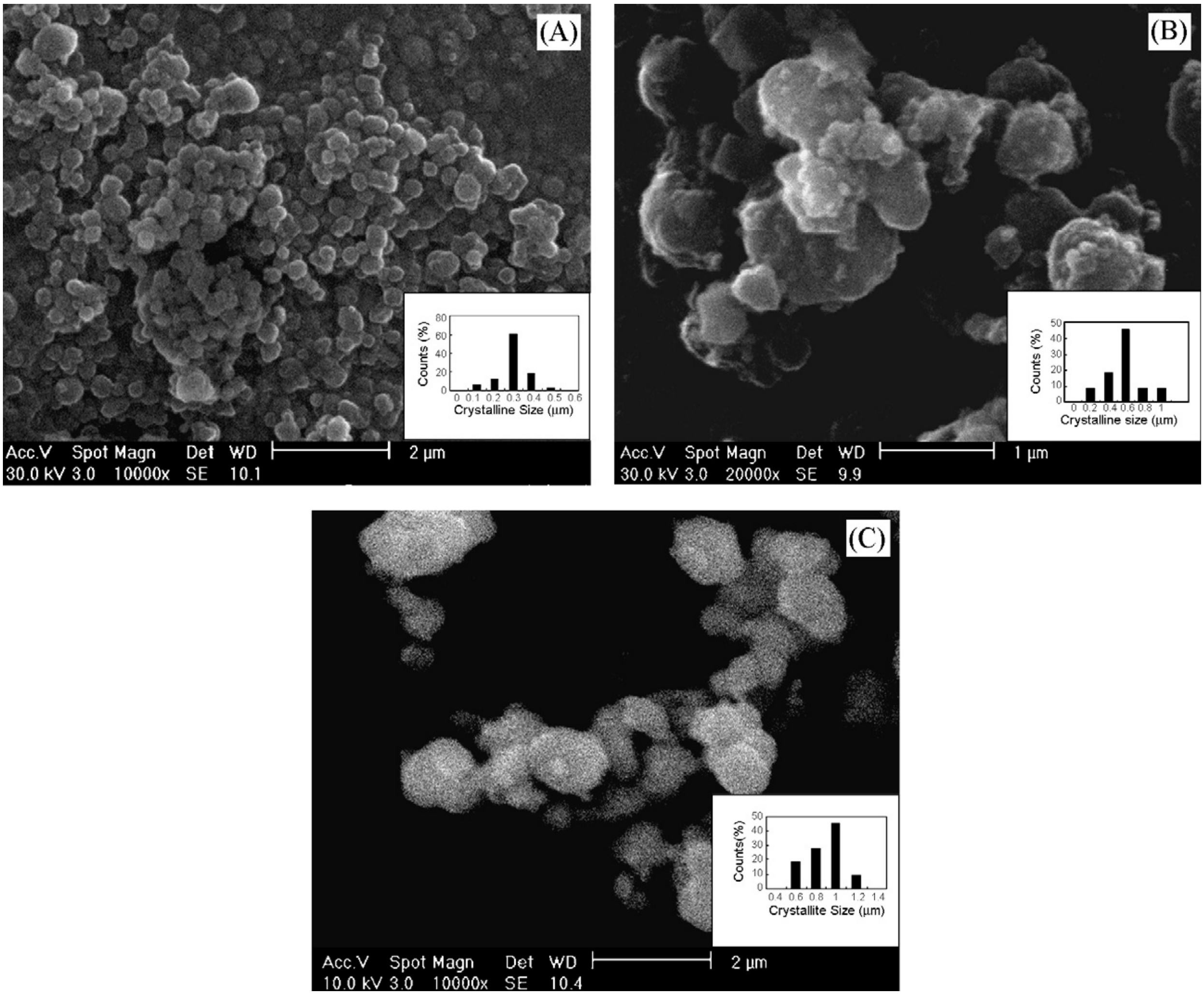

Fig. 2. Scanning electron micrograph of as-synthesized H-beta. (A) H-beta-1, (B) H-beta-2 and (C) H-beta-3.

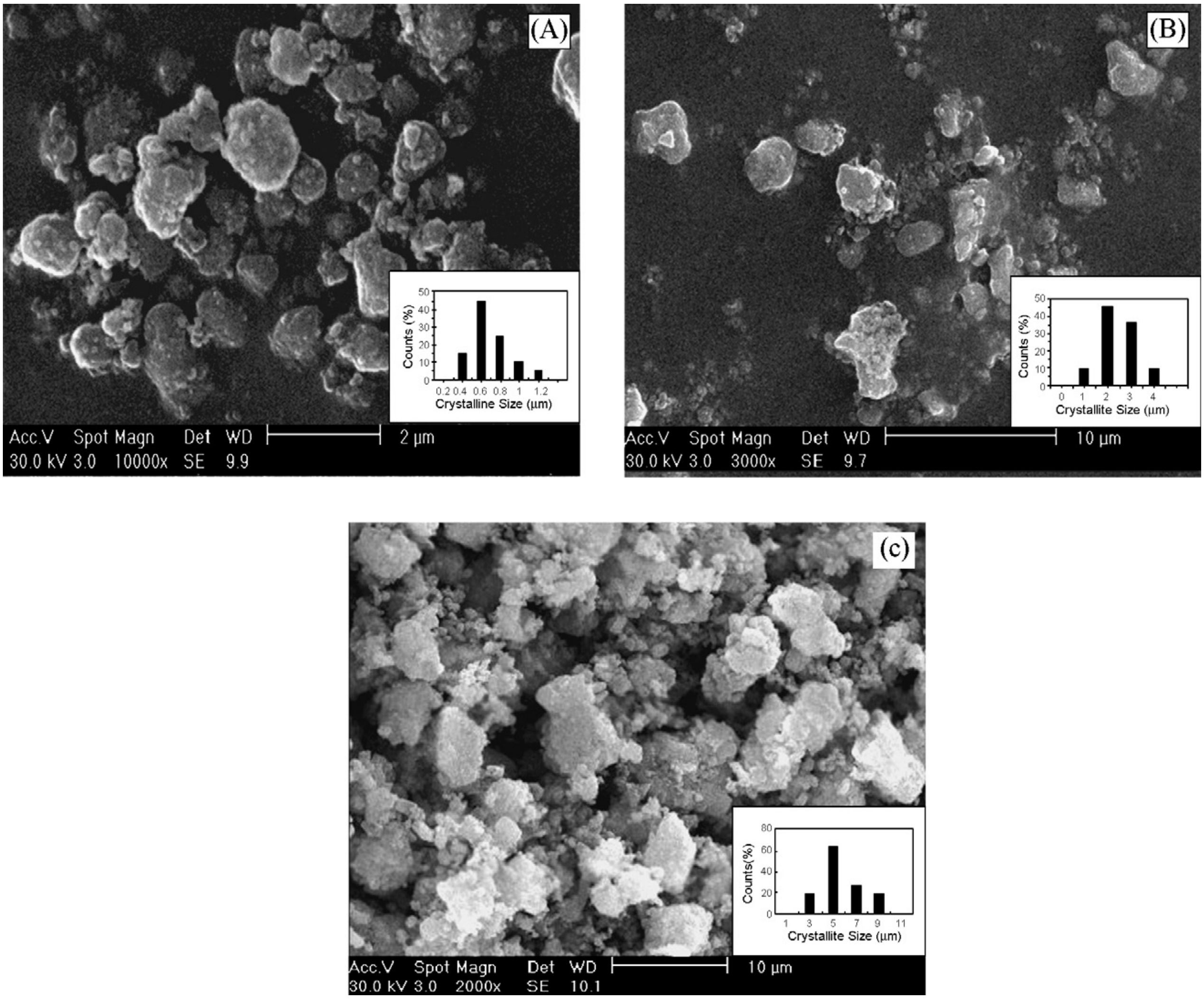

Fig. 3. Scanning electron micrograph of calcined H-beta. (A) H-beta-1, (B) H-beta-2 and (C) H-beta-3.

3.5. Effect of reaction temperature

Fig. 6 shows the effect of reaction temperature on the activity of H-beta-1. The conversion of HCHO increased quickly from 59.6% to 75.9% with the reaction temperature raised from 100 to 140 °C, and then increased slightly. At 180 °C, the conversion of HCHO reached 81.7%. The selectivity of *para–para*′-DMDPM kept nearly 85.0%, while the selectivity of 3-rings products increased at higher temperature.

3.6. Recycling of the catalyst

Table 5 summarized the results of the recycled H-beta-1. In these experiments, the catalyst was filtered off and washed with acetone, and activated at 550 °C for 3 h in the presence of air. The detected conversion of HCHO decreased only slightly after each recycle, the selectivity of DMDPMs and the *para–para*′-DMDPM are similar to that of the fresh catalyst. X-ray diffraction patterns (Fig. 7) of the five cycled H-beta-1 indicate

Table 4
Conversion and selectivity of DMPMs from toluene and HCHO over different sized H-beta

Zeolites	Conversion of		Particle size (μm)		Selectivity (on the basis of HCHO) (mol%)[c]			
	HCHO (%)	Toluene (%)			*Ortho–ortho*′	*Ortho–para*′	*Para–para*′	3-Rings
H-beta-1	75.9	10.1	0.3[a]	0.6[b]	1.1	10.3	86.5	2.1
H-beta-2	49.0	6.4	0.6[a]	2.5[b]	0.8	5.7	86.3	7.2
H-beta-3	56.7	7.4	1.0[a]	5.0[b]	2.1	6.0	85.3	6.6

Reaction conditions: zeolite 2.0 g; toluene 450 mmol; HCHO 30 mmol; reaction time 4 h and 140 °C.

[a] As-synthesized H-beta.

[b] After calcination at 550 °C for 3 h.

[c] Selectivity of DMDPMs = (mol of DMDPMs)/(total mol of DMDPMs +2 × mol of 3-rings products) × 100%.

that this sample retains a perfect crystallize structure as fresh sample.

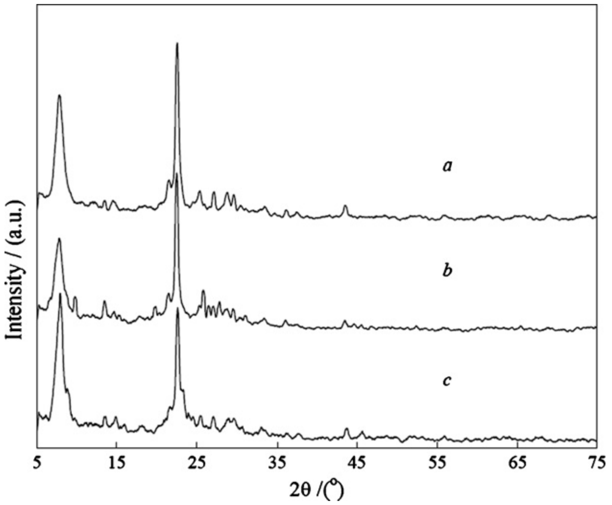

Fig. 4. XRD patterns of three H-beta after calcination at 550 °C for 3 h. (a) H-beta-1, (b) H-beta-2 and (c) H-beta-3.

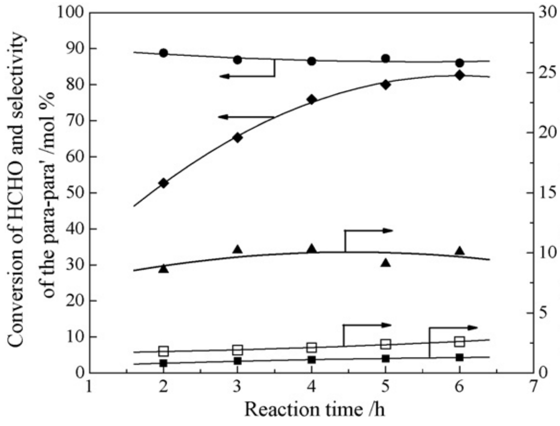

Fig. 5. Time course of condensation between toluene and HCHO over H-beta-1. (◆) Conversion of HCHO, (●) *para–para*′-DMDPMs, (▲) *ortho–para*′-DMDPMs, (■) *ortho-ortho'*-DMDPMs and (□) 3-rings product. Reaction conditions: H-beta-1 2 g; toluene 450 mmol; HCHO 30 mmol and 140 °C.

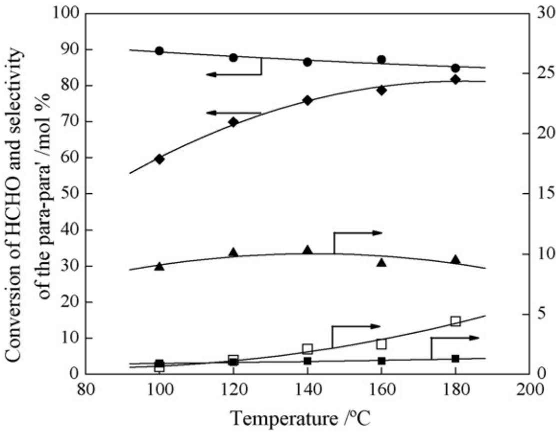

Fig. 6. Condensation between toluene and HCHO at different temperature over H-beta-1. (◆) Conversion of HCHO, (●) *para–para*′-DMDPMs, (▲) *ortho–para*′-DMDPMs, (■) *ortho-ortho'*-DMDPMs and (□) 3-rings product. Reaction conditions: H-beta-1 2.0 g; toluene 450 mmol; HCHO 30 mmol and 4 h.

Table 5
Recycling of H-beta-1

Runs	Conversion of		Selectivity (on the basis of HCHO) (mol%)[a]			
	HCHO (%)	Toluene (%)	*Ortho–ortho*′	*Ortho–para*′	*Para–para*′	3-Rings
1	75.9	10.1	1.1	10.3	86.5	2.1
2	74.8	9.9	1.1	10.9	86.7	1.3
3	74.5	9.9	0.9	9.9	88.1	1.1
4	73.5	9.8	0.9	10.2	87.6	1.3
5	73.4	9.7	1.1	9.3	88.1	1.5

Reaction conditions: H-beta-1 zeolite 2.0 g; toluene 450 mmol; HCHO 30 mmol; reaction time 4 h and 140 °C.

[a] Selectivity of DMDPMs = (mol of DMDPMs)/(total mol of DMDPMs + 2 × mol of 3-rings products) × 100%.

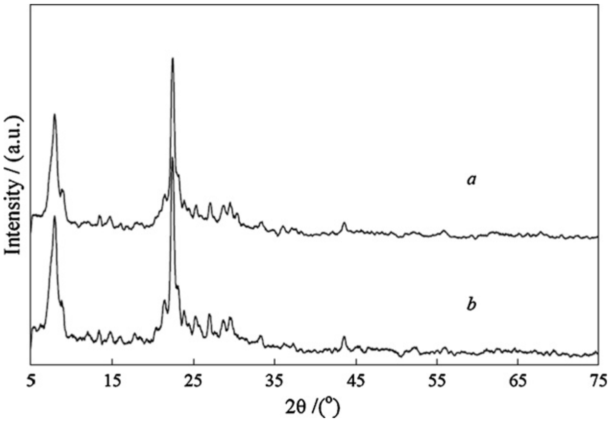

Fig. 7. XRD patterns of fresh and recycled H-beta-1. (a) Fresh H-beta-1 and (b) recycled H-beta-1.

4. Conclusion

In this paper, directly synthesis of *para–para*′-DMDPM via condensation between toluene and formaldehyde over H-beta was performed. Small sized H-beta zeolite was more active and exhibited a higher stereo-selectivity (>80%) even at higher temperature, longer reaction time and recycle usage. The best yield of *para–para*′-DMDPM reached 71.1% at 140 °C over H-beta zeolite and it could be used in recycle without loss of its structure, activity and stereo-selectivity.

Acknowledgements

This project is supported by National Natural Science Foundation of China (90610002) and Zhejiang Provincial Natural Science Foundation (Z406142, 2005C21048).

References

[1] R. Commandeur, N. Berger, P. Jay, J. Kervennal, European Patent 0442986 (1991).
[2] M. Akatsu, H. Takayama, European Patent 0428081B1 (1990).
[3] Y. Izumi, N. Natsume, H. Takamine, J. Tamaoki, K. Urabe, Bull. Chem. Soc. Jpn. 62 (1989) 2159.

[4] R.A. Sheldon, H. van Bekkum (Eds.), Fine Chemicals Through Heterogeneous Catalysis, Wiley–VCH, Weinheim, Germany, 2001.
[5] Y. Izumi, K. Urabe, M. Onaka, Zeolite, Clay Heteropoly Acid in Organic Reactions, Kodansha Ltd., Tokyo, Japan, 1992.
[6] A. Corma, Chem. Rev. 97 (1997) 2373.
[7] A. Corma, H. Garcia, Chem. Rev. 103 (2003) 4307.
[8] Z.Y. Hou, T. Okuhara, Chem. Commun. (2001) 1686.
[9] A.P. Singh, Catal. Lett. 16 (1992) 431.
[10] M.N. Timofeeva, G.M. Maksimov, V.A. Utkin, V.A. Likholobov, Kinet. Catal. 41 (2000) 767.
[11] S.N. Koyande, R.G. Jaisswal, R.V. Jayaram, Ind. Eng. Chem. Res. 37 (1998) 908.
[12] W. Hua, Y.H. Yue, Z. Gao, J. Mol. Catal. A 170 (2001) 195.
[13] A.P. Singh, B. Jacobb, S. Sugunan, Appl. Catal. A 174 (1998) 51.
[14] A. Corma, P. Botella, C. Mitchell, Chem. Commun. (2004) 2008.
[15] A. Cornelis, C. Dony, P. Laszlo, K.M. Nsunda, Tetrahedron Lett. 34 (1993) 529.
[16] K.B. Sherly, T. Bhat Venugopal, React. Kinet. Catal. Lett. 75 (2002) 239.
[17] Z.Y. Hou, T. Okuhara, Appl. Catal. A 216 (2001) 147.
[18] Z.Y. Hou, T. Okuhara, J. Mol. Catal. A 206 (2003) 121.
[19] D.F. Jin, Z.Y. Hou, Y.M. Luo, X.M. Zheng, Catal. Lett. 102 (2005) 109.
[20] D.F. Jin, Z.Y. Hou, Y.M. Luo, X.M. Zheng, J. Mol. Catal. A 243 (2006) 233.
[21] M.A. Camblor, J. Perez-Pariente, Zeolites 11 (1991) 202.
[22] R. Schmidt, D. Akporiaye, M. Stocker, O.H. Ellestad, J. Chem. Soc., Chem. Commun. (1994) 1493.
[23] S.G. Hegde, R. Kumar, R.N. Bhat, P. Ratnasamy, Zeolites 9 (1989) 231.
[24] M. Niwa, S. Nishikawa, N. Katada, Microp. Mesop. Mater. 82 (2005) 105.
[25] G.H. Kuehl, H.K.C. Timken, Microp. Mesop. Mater. 35–36 (2000) 521.
[26] M. Camiloti, S.L. Jahn, N.D. Velasco, L.F. Moura, D. Cardoso, Appl. Catal. A 182 (1999) 107.
[27] M.J. Climent, A. Corma, H. Garcia, J. Primo, Appl. Catal. 51 (1989) 113.
[28] J.M. Newsam, M.M.J. Treacy, W.T. Koestsier, C.B. de Gruyter, Proc. R. Soc. Lond. A 420 (1988) 375.
[29] J. Perez-Pariente, J.A. Martens, P.A. Jacobs, Zeolites 8 (1988) 46.
[30] Ch. Baerlocher, W.M. Meier, D.H. Olson, Atlas of Zeolite Framework Types, fifth revised ed., Elsevier, Amsterdam, 2001.